6 DOF Simulations for Stability Analysis of a Hydrofoil Towed by Kite

Nedeleg Bigi[1], nedeleg.bigi@ensta-bretagne.org
Kostia Roncin[1], kostia.roncin@ensta-bretagne.fr
Jean-Baptiste Leroux[1], jean-baptiste.leroux@ensta-bretagne.fr
Richard Leloup[2], richard.leloup@ensta-bretagne.org
Christian Jochum[1], christian.jochum@ensta-gretagne.fr
Yves Parlier[2], yves.parlier@beyond-the-sea.com

Abstract. Boats towed by kite, have currently great prospects. To better understand this technology in terms of loads, performance and stability, a 6 degrees of freedom simulator of a hydrofoil towed by kite with parametric modelling has been developed. Equilibrium states are found by using PID controller to simulate crew actions. This article investigates the flight stability of a dinghy boat towed by kite, the Skyboat® *3X*, with a rudder and with a canting dagger board, which both have a T-foil at their tip. The study focuses on the influence of two design parameters on the altitude stability: the size of the T-foil dagger board with a constant aspect ratio Λ and the dagger board cant angle ϕ_{DB}. From an equilibrium state, a perturbation is imposed on the T-foil rudder angle by a unit step function. Among the parameters (ϕ_{DB}, λ) tested, three types of responses have been identified: unstable, bounded and damped oscillatory. Then with the parameters (ϕ_{DB}, λ) conducting to damped oscillatory responses, the influences of (ϕ_{DB}, λ) on the static gain, overshoot, settling time and natural period are studied. Static gain and overshoot are mainly dependent on the dagger board cant angle, whereas settling time and natural period are dependent on both dagger board cant angle and T-foil dagger board size.

NOMENCLATURE

A_k	Kite surface
B	Beam
b	Span
C_B	Block coefficient
C_D	Drag coefficient
C_f	Skin friction coefficient
C_L	Lift coefficient
c	Chord length
c_M	Mean chord length
D	Drag force
$D_{\%}$	Percentage overshoot
DB	Subscript denoting dagger board
F	Subscript denoting Floater
h	Subscript denoting hull
I_{yy}	Pitch moment of inertia
I_{zz}	Yaw moment of inertia
k	Subscript denoting kite, form factor
KG	Height of center of gravity
K_s	Static gain
L	Lift force, length
L_{CG}	Longitudinal centre of gravity
L_{OA}	Length overall
L_P	Pole length
N	Yaw moment
N'	Non-dimensional yaw moment
$Pole$	Subscript denoting Pole
R_e	Reynolds number
R_T	Total resistance
RU	Subscript denoting rudder
R,TF	Subscript denoting T-foil at the root
r	Yaw velocity, subscript denoting derivative with respect to yaw velocity
$\dot{r}$	Yaw acceleration, subscript denoting derivative with respect to yaw acceleration
S	Appendage surface
T	Draught
$\hat{T}$	Period
T_k	Kite towing force
T,TF	Subscript denoting T-foil at the tip
TF	Subscript denoting T-foil
T_0	Natural period
U	Fluid velocity
U_0	Characteristic boat speed
V_A	Apparent wind velocity on kite
V_S	Hydrofoil advance speed
V_{WT}	True wind velocity
v	Sway velocity, subscript denoting derivative with respect to sway velocity
$\dot{v}$	Sway acceleration, subscript denoting derivative with respect to sway acceleration
WL	Subscript denoting waterline
x_{DB}	Dagger board longitudinal position from the stern
Y	Sway force
Y'	Non-dimensional sway force
α	Angle of attack
Δ	Displacement
$\Delta\theta_{TFRU}$	Step function amplitude
δ_{RU}	Rudder angle
ε_k	Kite drag-lift ratio
θ	Trim angle
θ_{TFRU}	T-foil rudder angle
Λ	Effective aspect ratio
Φ	Heel angle
Φ_k	Kite azimuth angle
ρ_{air}	Mass density of air
ρ_w	Mass density of sea water
ψ	Angle of yaw, heading or course
ψ_{pole}	Pole orientation angle

[1] ENSTA Bretagne – LBMS, France
[2] Beyond the Sea , France

1. INTRODUCTION

1.1 Context

To develop the skyboat® concept, a boat towed by a kite, the *beyond the sea*® project in partnership with the laboratory *LBMS* of *ENSTA Bretagne* currently develops a 6 Degrees Of Freedom (DOF) simulator of a hydrofoil towed by kite. This concept has great prospects both sportingly and economically. Indeed R. Leloup [1] showed that the implantation of a kite, as auxiliary propulsion device for a merchant ship, could generate fuel savings up to *26%* on a United States – France route. Sportingly, the main advantage that offers kite traction is that heeling moment due to aerodynamic forces is not a global sizing limit. So the righting moment is not the main feature determining the power of the boat and by extension the boat speed. But with the lack of global expertise of boats towed by kite, compared to sail boats with classical rig, the development of a 6 DOF simulator can provide a useful tool to handle the dynamic balance of forces.

Simulators currently called Dynamic Velocity Prediction Programs (DVPP) on classic sail boats are not a recently new domain of research. Step by step time domain simulations have been introduced to study the dynamic effect on boats performances. Larsson [2] in 1990 is the first to create a DVPP dedicated to design. Manoeuvers dynamic simulation of sailing yachts has been a scientific issue introduced for the first time by Masuyama et al. [3] in 1994 and reintroduced by J. A. Keuning et al. [4] in 2005, Verwerft et al. [5], and Binns et al. [6] in 2008. A match racing application which implied a 6 DOF simulator of two boats and their interactions was proposed by Roncin et al. [7] in 2004. Based on these previous developments, the present simulator aims to investigate the stability of a hydrofoil towed by kite (cf. Figure 1). The simulator has been implemented in a modular way, within the Matlab Simulink development environment. In this framework, the simulator can be improved easily by implementing new methods to calculate every single component. The special feature of this study is that the coupling with the kite has been modelled.

Firstly implementations and parametric models will be presented. Then results for a heave stability study will be presented and discussed. The study will be focused on the influence following design parameters:

- Dagger board cant angle
- T-foil dagger board size conserving the same geometric aspect ratio

1.2 Case study: the skyboat® 3X

The 3X is a single handed dinghy boat. The hull design is based on an International foiling moth shape. The 3X is equipped with a rudder and a canting dagger board. The two appendages both have at their tip a T-foil. The specificity of skyboat® is that they have a pole which can rotate on a complete revolution around the vertical axis of the boat. The kite tethers pass through a traveller along this pole.

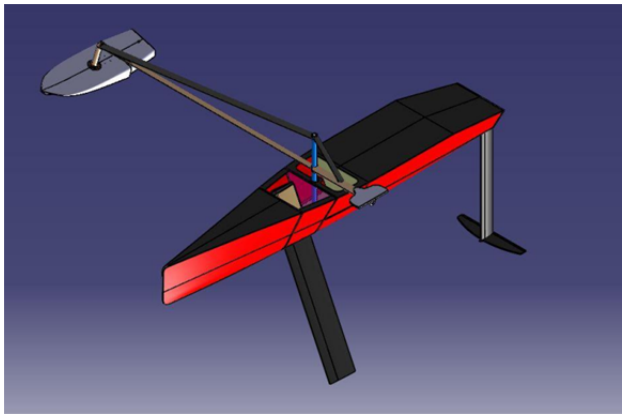

Figure 1. 3D view of the skyboat® 3X (without T-foil dagger board)

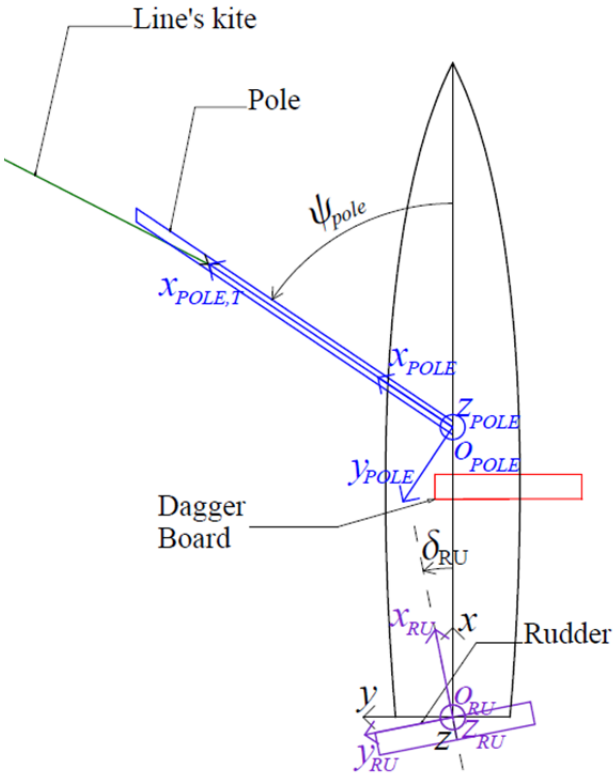

Figure 2. (x,y) schema of the 3X

The principle of this design is that the position of the traveller allows trimming the heel of the boat (cf. Figure 2). Altitude stability is expected to be given by the difference of cant angle between the dagger-board and rudder (cf. Figure 3). T-foil rudder angle of attack is adjustable to trim the altitude of the boat (cf. Figure 4). Indeed, if the boat gains in altitude, lifting dagger board area decreases, at the same time dagger board angle of attack and drift must increase for a given constant side force driven by the towing kite. Thus the T-foil dagger board angle of attack decreases because of the drift and altitude increase. An altitude increase produces a loss of

lift force for constant side force. Alternatively, an altitude decrease induces an increase angle of attack on the dagger board and therefore an increase in lift force.

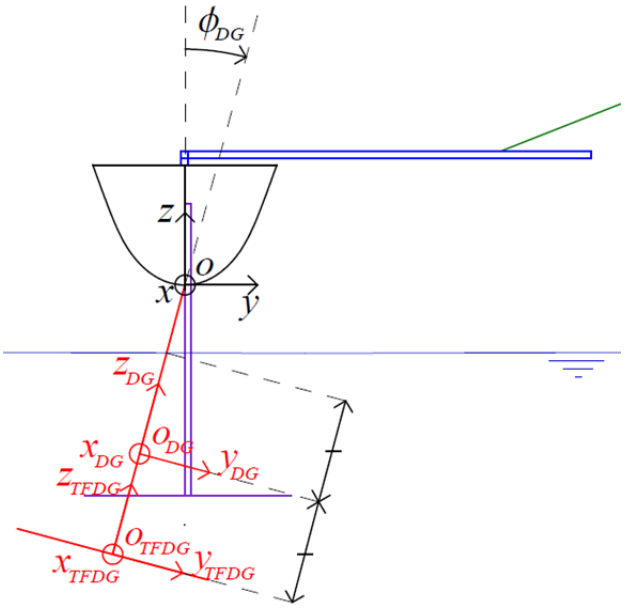

Figure 3. (Z,Y) schema of the 3X

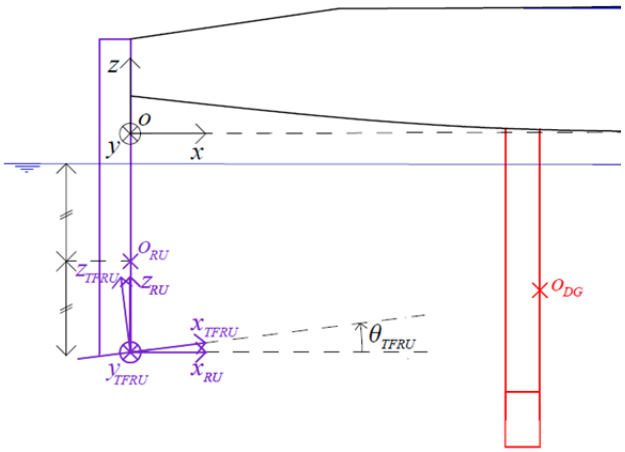

Figure 4. (X,Z) schema of the 3X, with $\delta_{RU} = 0°$

Boat specifications are listed in
Table **1**. The yaw inertia has been measured by a bifilar suspension method. In a first approach, we used exactly the same method as the one described by Hinrichsen [8]. However, due to repeatability issues, it has been preferred to attach ropes at the bow and at the stern. Assumption that yaw inertia is equal to pitch inertia was made because it has been considered that the appendages have not a huge influence on it (compared to a keel) and that the hull can roughly be compared to an axisymmetric body. The assumption about roll inertia is even rougher and questionable. It has been made since the roll measurement case is a way more difficult from a practical point of view. Two vertical lines are attached at the stern and the bow of the boat to a structure above. The boat is putted aside of his equilibrium position in such a way that the boat gets a yaw oscillating movement. The oscillation period $\hat{T}$ is measured. Finally from Newton's law the yaw inertia can be calculated by the following formula:

$$I_{zz} = \frac{\Delta}{4\pi^2}\hat{T}^2\left(\frac{(L-L_{CG})^2}{l_1}+\frac{L_{CG}^2}{l_2}\right) \qquad (1)$$

Where, l_1 and l_2 are the line's length respectively hanged at the bow and at the stern. It has been assumed roughly that the pitch inertia almost equals yaw inertia and roll inertia almost equals a tenth of yaw inertia.

	Parameters	Value	Unit
Hull	L_{OA}	*3.43*	*m*
	B	*0.7*	*m*
	δ	*27*	*Kg*
	L_{CG}	*1.53*	*m*
	KG	*0.13*	*m*
	I_{xx}	*3.2*	$N.m.s^{-2}$
	I_{yy}	*32.22*	$N.m.s^{-2}$
	I_{zz}	*32.22*	$N.m.s^{-2}$
Rudder	b_R	*0.97*	*m*
	$c_{M,RU}$	*0.12*	*m*
	Δ_{RU}	*2.78*	*Kg*
T-foil Rudder	b_{TFRU}	*0.83*	*m*
	$c_{R,TFRU}$	*0.125*	*m*
	$c_{T,TFRU}$	*0.05*	*m*
Dagger Board	b_{DB}	*1.13*	*m*
	$c_{M,DB}$	*0.13*	*m*
	Δ_{DB}	*4.0*	*Kg*
	x_{DB}	*1.13*	*m*
Pole	L_{Pole}	*2.0*	*m*
	Δ_{Pole}	*5.88*	*Kg*
Floater	Δ_F	*2.47*	*Kg*

Table 1. Skyboat® 3X specifications

2. MODELS OF THE SIMULATOR

In a first step, all models describing the forces acting on the boat should be simple to lead parametric studies.

The simulator solves Newton's laws of motion applied to a dinghy boat for the 6 degrees of freedom. The numerical scheme used to solve the 6 DOF dynamical system is the variable step 4th order Runge-Kutta scheme (ode45 Matlab routine). The integration is performed with a relative tolerance about the results of 10^{-6}. Time step convergence has also been checked through the use of fixed step 3rd and 4th order Runge-Kutta (ode3 and ode4 Matlab routines). The fact that all models are

parametric enables a modelling of the influence of the attitudes of the hull, since actual position parameters were taken into account at each time step.

2.1 Hydrodynamics Forces

Forces on the lifting appendages are calculated from the theory of wings [9].

$$L = \frac{1}{2}\rho_w S U^2 C_L \tag{2}$$

$$D = \frac{1}{2}\rho_w S U^2 C_D \tag{3}$$

The value of the lifting coefficient, C_L, is obtained from Helmbold's formula:

$$C_L = \frac{2\pi \cdot \Lambda \cdot \sin(\alpha)}{\sqrt{\Lambda^2 + 4} + 2} \tag{4}$$

Where, Λ is the effective aspect ratio and α is the angle of attack measured at the centre of the considered appendage. Effective aspect ratio Λ is used for dagger board and rudder considering that the mirror effect is done by the T-foil. For both T-foils, the geometric aspect ratio is considered because there is no mirror effect. The so-called mirror effect due to free surface or hull is also neglected as the Froude Number is high and the hull is supposed to be flying over the sea surface.
The drag coefficient C_D, takes into account a friction part derived from the ITTC57 formula:

$$C_f = \frac{0.075}{(\log_{10}(R_e) - 2)^2} \tag{5}$$

The Reynold's number is calculated with boat's speed and the chord length of each lifting profile. Then the drag coefficient is equal to:

$$C_D = \frac{C_L^2}{\Lambda\pi} + C_f \tag{6}$$

Considering the hydrostatic force,

$$\vec{\Delta} = -\rho_w \cdot T_h \cdot L_h \cdot B \cdot C_B \cdot \vec{g} \tag{7}$$

T_h and L_h are evaluated according to the following formulas with

$$T_h = \min(T_0, T_0 - x_G \sin(\theta)) \tag{8}$$

$$L_h = \min\left(L_{WL}, abs\left(\frac{T}{\tan(\theta)}\right)\right) \tag{9}$$

The manoeuvrability model implemented in the simulator is the one proposed by D. Clarke [10] formulated in his first order. The sway force and the yaw moment are given following formulas:

$$\begin{cases} Y = q \cdot L_{WL}^2 \cdot Y' \\ N = q \cdot L_{WL}^3 \cdot N' \end{cases} \tag{10}$$

Where the dimensionless forces and moment Y' and N' are given by:

$$\begin{cases} Y' = Y'_v \cdot v' + Y'_r \cdot r' + Y'_{\dot{r}} \cdot \dot{r}' + Y'_{\dot{v}} \cdot \dot{v}' \\ N' = N'_v \cdot v' + N'_r \cdot r' + N'_{\dot{r}} \cdot \dot{r}' + N'_{\dot{v}} \cdot \dot{v}' \end{cases} \tag{11}$$

The running resistance evolution with boat speed is provided by C. W. Prohaska in [11], from where it can be derived that the running resistance increases as $\left(\frac{U}{U_0}\right)^6$, assuming the wave resistance dominates the friction one at high Froude Number:

$$R_T = -\rho_w \cdot a \cdot \Delta \cdot \left(\frac{U}{U_0}\right)^6 \tag{12}$$

Where the value of a is extracted from the ORC VPP documentation 2011 based on Gerritsma et al. [12]. a was found equal to 0.649 for a Froude number of 0.75, which corresponds to a characteristic boat speed of 4.5 m.s-1[1].

2.2 Aerodynamics Forces

The kite is modelled in a static state. The method to calculate the kite's forces, implemented in the simulator, is extracted from the *zero-mass model* of R. Leloup [13], Figure 5[3]. According to Newton's laws applied to the kite, and assuming that the mass of the kite is zero, the following system permits to access to the kite's forces:

$$\begin{cases} \overrightarrow{V_A} = \overrightarrow{V_{TW}} - \overrightarrow{V_S} \\ \overrightarrow{T_K} + \overrightarrow{L_K} + \overrightarrow{D_K} = \vec{0} \end{cases} \tag{13}$$

With:

$$\begin{cases} L_K = \frac{1}{2}\rho_{air} A_K V_A^2 C_L \\ D_K = \frac{1}{2}\rho_{air} A_K V_A^2 C_D = L_K \tan(\varepsilon_K) \end{cases} \tag{14}$$

By using lift and drag expressions, the tension on the line can be expressed as:

$$T_K = -\frac{L_K}{\cos(\varepsilon_K)} \tag{15}$$

[3] Please note that in Figure 5 the eight shaped blue trajectory corresponds to a dynamic kite flight. In static flight the kite is on the window's edge (red line) as denoted by point K.

Knowing that a kite is evolving on a quarter-sphere, its position can be defined in spherical coordinates and according to system (14) and equation (15) the kite's position is defined by following condition. :

$$\cos(\phi_K) = \pm\frac{\sin(\varepsilon_K)}{\cos(\theta_K)} \quad (16)$$

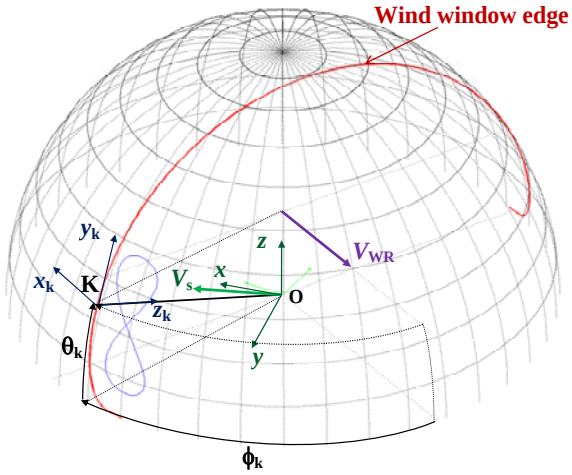

Figure 5. Flying kite within the wind window

The lift and drag coefficient are taken from experiments performed by G. Dadd [14] on a ram-air kite.

One of the main interests of the towing by kite is that the kite can be positioned high in the atmospheric boundary layer, where the wind is stronger and more consistent. Thus it is necessary to take into account the wind gradient effect on the kite forces calculation. According to ITTC [15], the wind velocity as a function of altitude can be calculated using the expression:

$$V_{WT} = U_{10}\left(\frac{z_K}{10}\right)^n \quad (17)$$

Where:

- U_{10} is the wind velocity at standard altitude $10\ m$, in $[m.s^{-1}]$
- z_K is the kite altitude above sea level in $[m]$
- n is a coefficient which is equal to 1/7 over the sea surface as specified by ITTC [13]

2.3 Controls: yaw, roll and altitude

Controls aim to simulate crew actions. They concern heading with angle of the rudder δ (Figure 2), heeling angle with the position of the traveller on the pole x_{pole} (Figure 2), and altitude with the angle of the T-foil rudder θ_{TFRU} (Figure 4). All these controls are made by the system's Proportional-Integral-Derivative controllers (PID).

3. ALTITUDE STABILITY STUDY

This study aims to investigate the dagger board cant angle ϕ_{DB} and the T-foil dagger board size influence on the boat heave stability. Note that the influence of the rake angle on the stability has not been studied since the skyboat® principle is to adjust the altitude with the T-foil rudder angle instead of the dagger board rake angle. In order to simplify the study, all T-foil dagger board configurations have the same geometric aspect ratio as the T-foil rudder. So let's introduce the length units describing the T-foil rudder and the T-foil dagger board, respectively l_{TFRU} and l_{TFDB} with the relation $l_{TFDB} = \lambda \cdot l_{TFRU}$. All lengths of T-foil dagger board are given by lengths of T-foil rudder in product with a scale coefficient λ. In summary, this study investigates effects of ϕ_{DB} and λ.

For all following numerical tests, the boat is towed by a kite of $10\ m^2$ with tethers of $30\ m$ and with an angle of elevation, $\theta_K = 20°$ (cf. Figure 5). The pole is oriented with an angle, $\psi_{pole} = 85°$(cf. Figure 2) from the bow. The true wind speed is $5\ m.s^{-1}$ at the altitude of $10\ m$. The true wind angle command is 90° and the heeling angle command is 0°.

3.1 Initialization

With all parameters fixed and for each couple (ϕ_{DB}, λ), the initialisation consists to find the correct boat attitude, boat velocity and T-foil rudder angle, θ_{TFRU} to fly at the altitude of $0.4\ m$ in a static equilibrium.

The process to determine this state of static equilibrium is achieved by a simulation of $40\ s$ during which yaw, roll and altitude are servo-controlled. In this way, the state is automatically determined at $40\ s$ (cf. Figure 6).

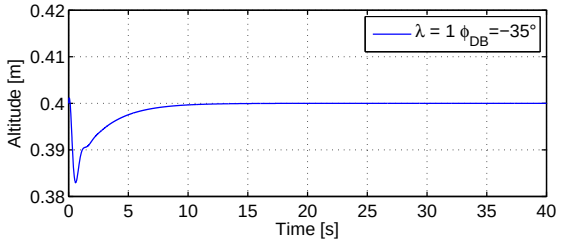

Figure 6. Altitude evolution simulated during an initialization step with $\phi_{DB} = -35°$ and $\lambda = 1$

3.2 Simulations with perturbation

Simulations with perturbation use states of static equilibrium for the altitude $0.4\ m$ determined during in the initialisation process. The perturbation is made by the T-foil rudder. The angle, θ_{TFRU} is increased at $20\ s$ by

$\Delta\theta_{TFRU} = 1°$ with the unit step function (cf. Figure 7).

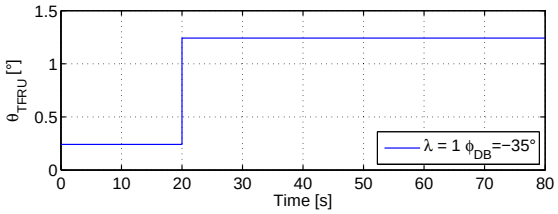

Figure 7. Perturbation signal evolution of T-foil rudder angle, θ_{TFRU}

Due to the temporal numerical scheme the unit step function is defined with a delay of $1.10^{-3}s$. Thus, the initial equilibrium is disturbed. And the study will focus on the ability to find another state of equilibrium.

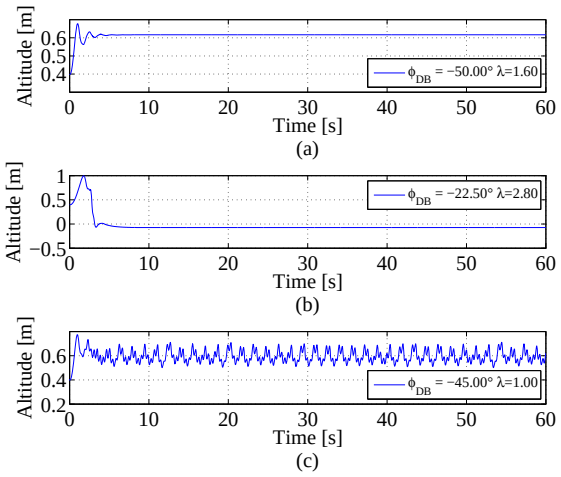

Figures 8-a,b,c. Altitude by time simulation during a perturbation process for three configurations of (ϕ_{DB}, λ)

In order to simplify the lecture of the Figures 8, time simulation is shifted, $t = 0\ s$ correspond to the beginning of the unit step function, instead of $t = 20\ s$ on Figure 7, and the simulation ends at $t = 60\ s$. Figures 8 shows three types of altitude response of the boat over time for different couples (ϕ_{DB}, λ) to the unit step function perturbation.

The Figures 8.a, obtained with a couple $(\phi_{DB}, \lambda) = (-50.00°, 1.60)$, corresponds to a damped oscillatory response. All configurations conducting to this type of responses are located in the area with red asterisks shown on Figure 9.

The Figures 8.b obtained with a couple $(\phi_{DB}, \lambda) = (-22.50°, 2.80)$, shows that after the perturbation the boat looses the flight state. The Figures 8.c, obtained with a couple $(\phi_{DB}, \lambda) = (-45.00°, 1.00)$, corresponds to a bounded oscillatory heave motion. These both cases are obtained for couple (ϕ_{DB}, λ) located in the area with blue cross shown on Figure 9.

For some configurations (ϕ_{DB}, λ) no flight equilibrium state are found during the initialization phase. Configurations qualified as unstable corresponds to couples (ϕ_{DB}, λ) which lead during the perturbation process to the boat jump out of the water. These both cases are obtained with couples (ϕ_{DB}, λ) located in the area with black circle shown on Figure 9.

Otherwise, different numerical schemes (3th and 4th order Runge-Kutta scheme in fixed step and 4th order in variable step) have been tested. All numerical schemes show exactly the same phenomenon, provided that sufficiently small fixed time steps are used for the ode3 and ode4 schemes. This verification leads to state that all results are related to the mathematical model.

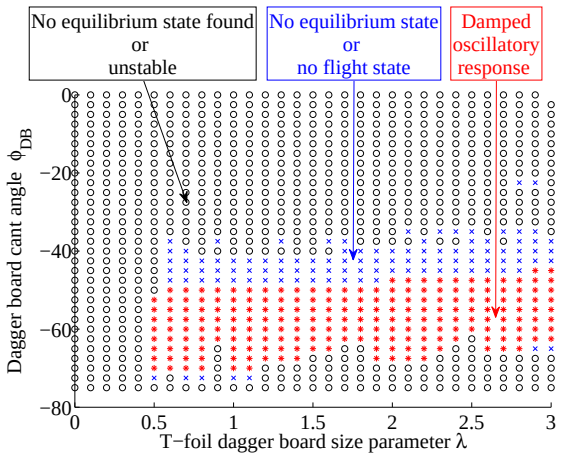

Figure 9. Boat heave stability response for several couples (ϕ_{DB}, λ); no equilibrium state found or unstable: black circle; No equilibrium state or no flight state: blue cross; damped oscillatory: red asterisk.

4. RESULTS

All following figures (Figure 10 to Figure 13) correspond to couples (ϕ_{DB}, λ) which lead to a damped oscillatory behaviour (couples from the area with red asterisks Figure 9). Figure 10 plots the surface representing the static gain K_s of the system versus (ϕ_{DB}, λ). The static gain is defined as follows:

$$K_s = \frac{z(t=60) - z(t=0)}{\Delta\theta_{TFRU}} \qquad (18)$$

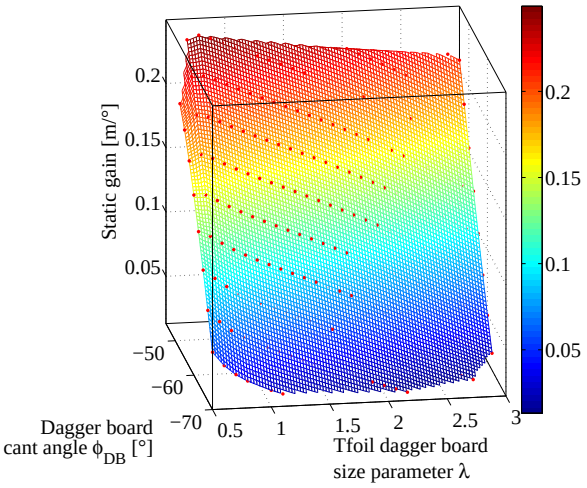

Figure 10. Static gain, K_s versus (ϕ_{DB}, λ)

Figure 11 is a plot of the overshoot, $D_{\%}$ versus (ϕ_{DB}, λ). The overshoot represents the maximum altitude value measured from the final value and is defined by following formula:

$$D_{\%} = \frac{z_{\max} - z(t=60)}{z(t=60)} \cdot 100 \qquad (19)$$

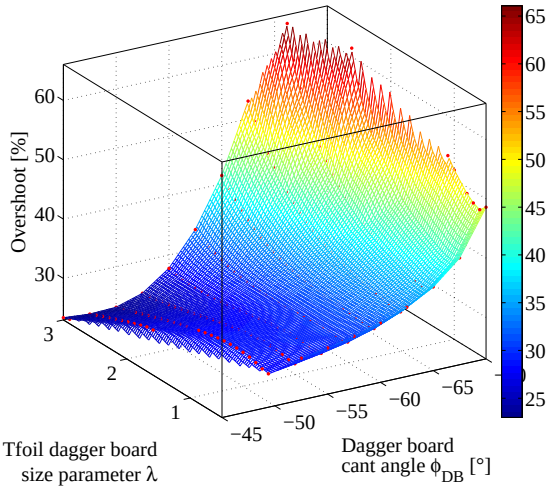

Figure 11. Overshoot, $D_{\%}$, versus (ϕ_{DB}, λ)

Figure 12 represents the settling time from the time when the unit step function is imposed to the time at which the boat altitude has entered and remained within the 5% error band of the final value.

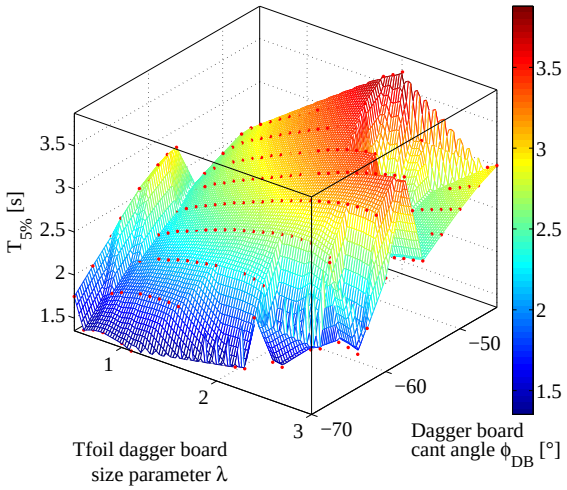

Figure 12. Settling time, $T_{5\%}$, versus (ϕ_{DB}, λ).

Figure 13 is a plot of the natural period of the system. The natural period is calculated by a measure of the time between the two first overshoots.

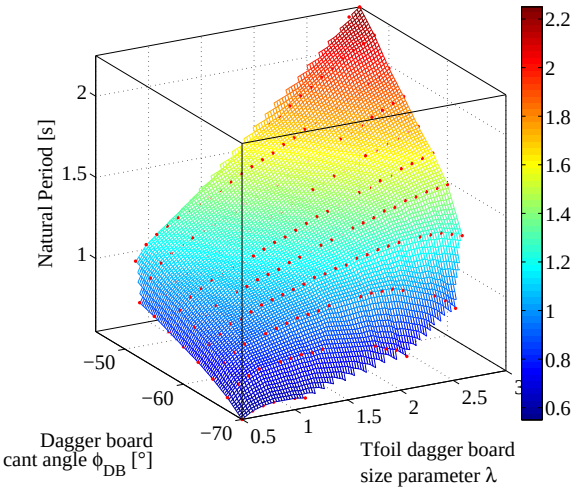

Figure 13. Natural period, T_0, versus (ϕ_{DB}, λ)

Figure 14 is a plot of the boat speed.

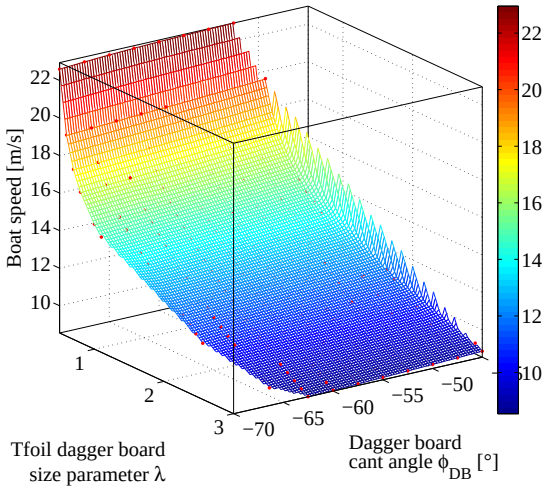

Figure 14. Speed versus (ϕ_{DB}, λ)

5. ANALYSE

Focusing on damped oscillatory responses (Figure 9 red asterisk), the damping effect explanation could be related to the appendages lift forces in accordance with the T-foil stability process (explained in the 2nd § of section 1.2). Indeed lifting forces depend on speed component perpendicular to foil planform which is by definition a damping term. So this means that the T-foil dagger board stability process exists within the meaning of the mathematical model.

To qualify the stability process and to distinguish design configuration, static gain (cf. Figure 10), percentage overshoot (cf. Figure 11), settling time to 5% (cf. Figure 12) and natural period (cf. Figure 13) have been plotted against parameters (ϕ_{DB}, λ)

On Figure 10, static gain seems to be rather close to a linear function depending on (ϕ_{DB}, λ). Static gain increases with a decreasing of the absolute value of the dagger board cant angle, $|\phi_{DB}|$ and a decreasing of the T-foil dagger board size parameter λ. It can be noticed that $|\phi_{DB}|$ have more influence on the static gain than λ over the design range of (ϕ_{DB}, λ).

On Figure 11 the evolution of the overshoot is more complex. Overshoot value is within a range $[25\%; 60\%]$. For all values of T-foil dagger board size parameter λ, a minimum overshoot is observable around $-50°$ of canting dagger board angle ϕ_{DB}. Overshoot does not vary a lot with parameter λ. For $\phi_{DB} = -50°$, overshoot is within a range of [24%;28%].

On Figure 12 settling time to 5% should be considered as an equivalent of a damping coefficient. Even if steps are observable, only the global variation should be considered. Indeed, steps are a direct consequence of the settling time to 5% definition. The settling time is broadly increased by the increasing of the T-foil dagger board size parameter λ and by a decreasing of the absolute value of dagger board angle $|\phi_{DB}|$.

Natural period (cf. Figure 13) of the system has the same evolution as the settling time to 5%. The natural period is within a range from less than $T_0 = 0.5\ s$ for a couple $(\phi_{DB}, \lambda) = (-67.5°, 0.6)$ to more than $T_0 = 2\ s$ for a couple $(\phi_{DB}, \lambda) = (-30°, 2.5)$.

Boat speed evolution with (ϕ_{DB}, λ) is mainly directed by the T-foil dagger board size λ. The smaller λ is, the faster is the boat.

6. DISCUSSION

For couples (ϕ_{DB}, λ) conducting to a damped oscillatory heave motion, the parametric study analyses four characteristics of the damped oscillatory responses: static gain, percentage overshoot, settling time to 5%, natural period and boat speed. Static gain and overshoot are mainly dependant of the dagger board cant angle ϕ_{DB}. Overshoot presents a particular feature, for a given t-foil dagger board size parameter λ, the overshoot is minimal around $\phi_{DB} = -50°$. By contrast, boat speed is mainly dependant on parameter λ. Settling time to 5% and natural period are all dependent on ϕ_{DB} and λ.

There is no ideal value of the design parameters (ϕ_{DB}, λ) to increase the altitude stability. However, one of the most obvious characteristic to decrease is the overshoot. Indeed, a too much important overshoot could be dramatic on the boat response and conducts the boat to a crash. Thus a dagger board cant angle around $-50°$ should be ideal to this point of view. Natural period of the system is important to take into account to avoid resonance periods shared between the dynamic flight and structural elements of the boat. Also, greater the natural period, smaller are the induced acceleration and so dynamic mechanical stresses. This means that high values of the T-foil dagger board size parameter λ are appropriated. However, the smaller λ is the faster is the boat. Therefore, no couple (ϕ_{DB}, λ) could be identified as better than another. But, this study shows that such a tool could be helpful for a naval architect in an early design stage.

Otherwise, the static gain settling time, provides relevant information to design an active control system to regulate the altitude of a foiling boat.

Of course all precedent results are under the control of the mathematical model and its validation still needs to be done. On the other hand, some important phenomena have not been modelled like windage on the boat and kite tethers. . Consequently, boat speed results on Figure 14 are expected to be over-estimated. The added mass induced by the appendages which seems to be important for particular unstable or transient configurations as

shown by the work of La Mantia and P. Danichki in ref [16], needs to be investigated too..

7. CONCLUSION

An altitude stability study has been conducted on a foiling boat towed by a kite with a parametric 6 DOF simulator. Finally, it has been shown that a unit step function perturbation on the angle of the T-foil rudder could conduct the 3X to four behaviours in altitude, unstable, loss of flight, bounded oscillatory and dampened oscillatory depending on the dagger board cant angle and T-foil dagger board size. The dampened oscillatory static gain and overshoot are mainly influenced by the dagger board cant angle whereas the settling time and natural period are influenced by both dagger board cant angle and T-foil dagger board size. The interest of such simulator is shown for early design and control system design.

References

1. R. Leloup, K. Roncin, G. Bles, J-B. Leroux, C. Jochum, and Y. Parlier. A novel modeling for performance assessment of kites as auxiliary propulsion device for merchant ships. *International Conference on Computer Applications in Shipbuilding*, 2013.
2. L. Larsson. Scientific methods in yacht design. *Annual Review Fluid Mechanics,* pp 349-383 1990
3. Y. Masuyama, T. Fukasawa and H. Sasagawa. Tacking Simulation of Sailing Yachts–Numerical Integration of Equations of Motion and Application of Neural Network Technique. *The 12th Chesapeake Sailing Yacht Symposium,* 1995.
4. J. A. Keuning, K. J. Vermeulen and E. J. de Ridder. A Generic Mathematical Model for the Maneuvering and Tacking of a Sailing Yacht. *The 17th Chesapeake Sailing Yacht Symposium*, 2005.
5. B. Verwerft and A. Keuning. The modification and application of a time dependent performance prediction model on the dynamic behaviour of a sailing yacht. *Proceeding of the 20th international hiswa symposium on yacht design and yacht construction*, 2008.
6. J. R. Binns, K. Hochkirch, F. De Bord and I. A. Burns. The Development and Use of Sailing Simulation for Iacc Starting Manoeuvre. *Training, in 3rd High Performance Yacht Design Conference,* 2008.
7. K. Roncin and J. M. Kobus. Dynamic simulation of two sailing boats in match racing. *Sports Engineering*, *7*(3), pp 139-152, 2004.
8. Peter F. Hinrichsen. Bifilar suspension measurement of boat inertia parameters. Journal of Sailboat Technology, Article 2014-01, The Society of Naval Architects and Marine Engineers, 2014
9. J-D. Anderson. Fundamentals of Aerodynamics. Third Ed. McGraw Hill, 2001.
10. D. Clarke, P. Gelding, and G. Hine. The application of manoeuvring criteria in hull design using linear theory. *The Naval Architect*, pp 45-68, 1983.
11. C. W. Prohaska. A simple method for the evaluation of the form factor and low speed wave resistance. *Proceedings 11th ITTC,* 1966.
12. Gerritsma, J., Keuning, J., & Versluis, A. (1993, January). Delft University of technology, Delft Netherlands,"Sailing yacht performance in calm water and in waves.". In Eleventh Chesapeake sailing yacht symposium, Annapolis, Maryland (pp. 233-246).
13. R. Leloup, K. Roncin, G. Bles, J-B. Leroux, C. Jochum, and Y. Parlier. Estimation of the lift-to-drag ratio using the lifting line method: application to a leading edge inflatable kite. *Airborne Wind Energy*, pp 339-355, 2013.
14. G. M. Dadd, A.D. Hudson and R. A. Shenoi. Comparison of two kite force models with experiment. *Journal of Aircraft* 47.1 212-224, 2010.
15. ITTC Symbols and Terminology List, 2011.
16. M. La Mantia, P. Dabnichki. Added mass effect on flapping foil. *Enginering Analysis with Boudary Elements* 36 579-590, 2012.